Journal of Applied Physics

Investigation of high harmonic generation from laser ablated plumes of silver

Cite as: J. Appl. Phys. **130**, 013101 (2021); https://doi.org/10.1063/5.0054337
Submitted: 16 April 2021 • Accepted: 11 June 2021 • Published Online: 02 July 2021

Srinivasa Rao Konda, Yu Hang Lai and Wei Li

Journal of Applied Physics ARTICLE scitation.org/journal/jap

Investigation of high harmonic generation from laser ablated plumes of silver

Cite as: J. Appl. Phys. **130**, 013101 (2021); doi: 10.1063/5.0054337
Submitted: 16 April 2021 · Accepted: 11 June 2021 ·
Published Online: 2 July 2021

Srinivasa Rao Konda,[1,a] Yu Hang Lai,[1,2,a] and Wei Li[1,2,a]

AFFILIATIONS

[1]GPL, State Key Laboratory of Applied Optics, Fine Mechanics and Physics, Chinese Academy of Sciences, Changchun Institute of Optics, Changchun 130033, China
[2]University of Chinese Academy of Sciences, Beijing 100049, China

[a]**Authors to whom correspondence should be addressed:** ksrao@ciomp.ac.cn, laiyh@ciomp.ac.cn, and weili1@ciomp.ac.cn

ABSTRACT

Silver (Ag) is one of the important targets in the studies of high harmonic generation (HHG) in the laser-induced plasma due to the relatively high conversion generation efficiencies and cut-off energy. In this work, we study the dependence of HHG in plasma plumes of Ag as a function of various laser parameters, including intensity of ablation pulse, intensity and ellipticity of driving pulse, and the delay between the two pulses. We identify the type of ion that dominates the measured HHG spectra by comparing the experimental data with strong-field approximation simulations and classical calculations for Ag atoms, Ag^+, and Ag^{2+} ions. We also perform a comparative HHG study between the plasmas of bulk Ag target and the plasmas of a nano-powders target. It is found that the harmonic yields in the latter case are higher over a wide range of the aforementioned laser parameters. The results also indicate that the number of nanoparticles in the plasma generated from a nano-powder sample is indeed significantly greater than that in the plasma from the bulk sample.

I. INTRODUCTION

High harmonic generation (HHG) from gaseous targets has been demonstrated to be an attractive method to generate ultrashort coherent radiation in the extreme ultraviolet spectral range and attosecond pulses.[1–5] Over the last 15 years, laser-induced plasma plumes produced from solid surfaces have been recognized as alternative media for HHG.[6–12] It has been found that the generation efficiencies and cut-off photon energies vary significantly among different target species, and interesting harmonic characteristics have been observed. Moreover, several types of metal ions give particularly strong intensity at some specific harmonic orders[13–15] due to their electron resonance properties.[16] Early plasma plume HHG studies focused on using pure bulk solid metals as the ablation targets. Recently, more complex targets have been used, such as compound[17] nanoparticles (NPs).[18–21] One of the challenges in the studies of plasma plume HHG is that it is often difficult to identify which components in the plasma (neutral atoms, ions of different charge states) contribute to HHG.

In this work, we present systematic investigations on HHG in plasma plumes of silver (Ag). Ag is one of the important targets for HHG because of the good generation efficiency and relatively high cut-off energy compared with many other metal targets.[22–27] We measured the HHG spectrum as a function of various laser parameters, including intensity of the heating pulse for ablation, intensity of the driving pulse, ellipticity of the driving laser, and the delay between the two pulses. By comparing the data with Lewenstein model simulations and classical calculations for Ag atoms, Ag^+ and Ag^{2+} ions, we infer which species dominate the measured harmonic spectra.

In addition to using plasma from the bulk Ag target, we also perform the same HHG measurements with plasma from a target composed of Ag NP target. We observed that the overall harmonic yield from the NP sample is consistently higher than the yield from the bulk sample over a wide range of the laser parameters. We also found that HHG from the NP target survives at larger values of the heating pulse–driving pulse (HP-DP) delay (and with higher yield) compared with the bulk sample, which is evidence that shows that the number of NPs in the plasma generated from the NP sample is indeed significantly greater than that in the plasma from the bulk sample.

II. EXPERIMENTAL DETAILS

The studies used a Ti: Sapphire chirped-pulse amplifier (CPA) system operating at 800 nm, 35 fs, with a repetition rate of 1 kHz as

the driving laser for HHG. The laser-induced plasma (LIP) is produced by irradiating the target surface with heating pulses (HPs) (i.e., the pulses used to create the plasma plumes by laser ablation of targets). Two types of HPs are used: nanoseconds (1064 nm, 5 ns) and picoseconds (800 nm, 200 ps) pulses. The nanosecond HPs are produced from a Nd: YAG laser, which is electronically synchronized to the CPA laser system, whereas the picosecond HPs are obtained simply by splitting a small fraction of the amplified laser pulse beam in the CPA system before temporal compression. The optically driven delays between the picosecond HP and femtosecond driving pulse (DP) originated from the same CPA system are fixed at 80 ns. However, in the case of nanosecond HP, the HP-DP delay is controlled electronically using an external delay generator (Stanford Research Instrument, DG535) triggered by the controller of the CPA system. In either case, the HPs were focused on the sample surface using a lens of a focal length of 200 mm ($1/e^2$ beam radius at a focus for picoseconds beam of 71 μm and nanoseconds of 34.5 μm). The DPs are focused using a lens with a focal length of 500 mm ($1/e^2$ beam radius at focus of 43.5 μm) propagating parallel to the sample surface and perpendicular to the propagation axis of the HPs, as shown in Fig. 1. The harmonic yield is optimized by adjusting the distance between the target and the optical axis of propagation of the DP and by varying the focal position of the HP. The generated harmonics emission enter an extreme ultraviolet (XUV) spectrometer which consisted of a cylindrical mirror and a 1200 grooves/mm flat field grating with variable line spacing. XUV signal is detected using a microchannel plate with a phosphor screen, and the fluorescent light on the screen is imaged by a CCD camera.

III. RESULTS AND DISCUSSION

The results and discussion of this paper contain two parts: the first part describes the experimental and theoretical calculations of HHG from the LIP of the bulk Ag target with various laser parameters including the intensity of HP, intensity, and ellipticity of DP. The experimental data are recorded using ps HPs. In the second part, we compare HHG in the LIP of bulk Ag and the LIP of nanopowders as a function of the laser parameters considered in the first part. We also use the ns HPs to investigate the dependences of harmonic yield on the HP intensity and the delay between the HP and DP.

A. Harmonic's spectra produced from LIP of bulk Ag and theoretical simulations

The 2D color plot in Fig. 2(a) shows the HHG spectra generated from the Ag plasma as a function of DP intensity. The ps HP intensity (I_{ps}) is fixed at 7.4×10^9 W/cm^2. The lower-order harmonics in HHG spectra are stronger at a low DP intensity, whereas the overall harmonic yield increases with the DP intensity. It is observed that as the DP intensity (I_{fs}) reaches 2.4×10^{14} W/cm^2 or higher, the spectrum possess a plateau-like pattern from 13H to 43H. It should be noted that the plasma plumes usually contain ions of different charge states and, in principle, they could all contribute to the measured harmonic spectra. Currently, we do not have the experimental capability to perform *in situ* measurements of the spatial–temporal distribution of the densities of different ions in the plasma plumes. Nevertheless, from calculations, we could estimate on the contributions from ions of different charge

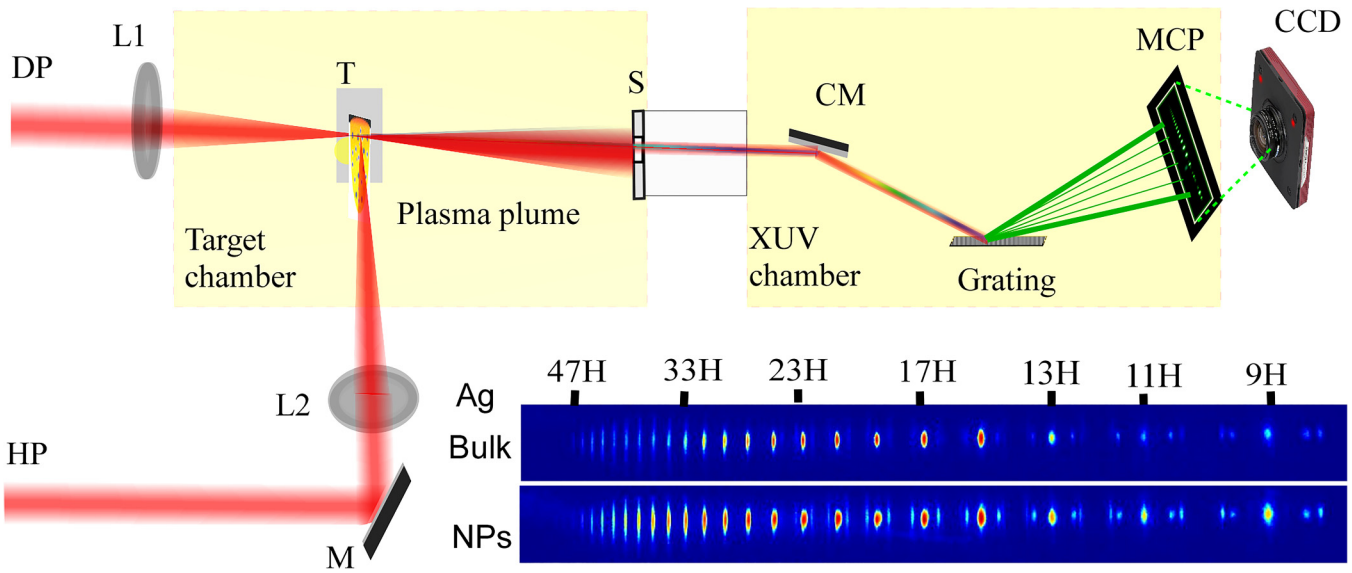

FIG. 1. Experimental setup for high order harmonic generation, from laser-induced plasma of targets (T: Ag bulk, 20 nm NPs), DP: driving pulse 800 nm, 35 fs, HP: heating pulse, 200 ps (800 nm), and 6 ns (1064 nm), L1–L2: lens, corresponding focal lengths f_1 = 500 mm, f_2 = 200 mm, respectively. S: slit, CM: cylindrical mirror, MCP: microchannel plate. The color panel shows HHG spectra at a driving pulse intensity of 4.5×10^{14} W/cm^2, ps HP intensity of 6.0×10^9 W/cm^2, for bulk and NPs.

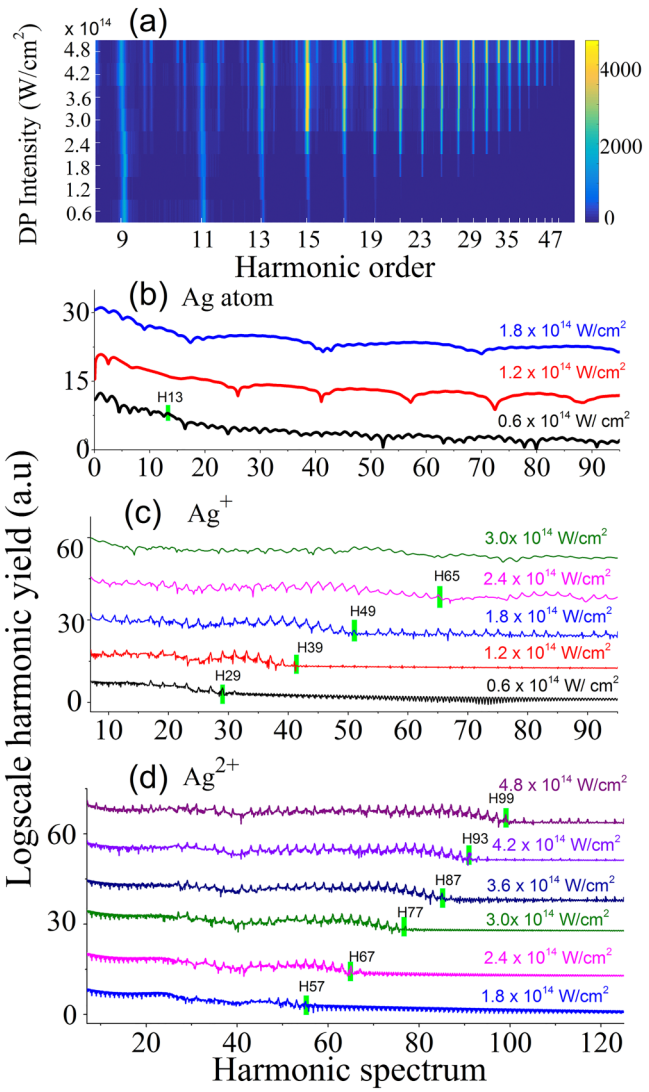

FIG. 2. (a) 2D color map of HHG spectra for various DP intensities within the range of 0.6×10^{14} W/cm^2 to 4.8×10^{14} W/cm^2 for Ag bulk, at $I_{ps} = 7.4 \times 10^9$ W/cm^2. Calculated HHG spectra at different DP intensities for (b) Ag atoms, (c) Ag^+ ions, and (d) Ag^{2+} ions. For visibility, each spectrum is displaced from the other vertical by an arbitrary unit.

states. Using the Perelomov–Popov–Terent'ev (PPT) formula of ionization rate[28] (which is applicable for ionization in both multi-photon and tunneling regime)[29] to estimate the ionization probabilities of neutral Ag atoms, Ag^+ ions and Ag^{2+} ions, it is found that the ionization probability of Ag and Ag^+ approaches 100% (saturation) when the laser intensity reaches 2×10^{13} and 2.5×10^{14} W/cm^2, respectively. As for Ag^{2+}, the ionization probability is still only about 4% at the highest DP intensity in our experiment. At first sight, one might expect that the measured harmonics spectra should be dominated by the contributions from neutral Ag and Ag^+ due to their high ionization probabilities. But, if the ionization process saturates too rapidly (that is, the ground state population is depleted way before the atom/ion experiences the central peak portion of the laser pulse), the HHG process would become ineffective. Recall that from Lewenstein model,[30] HHG is a three-step process: (i) ionization by the strong laser field, (ii) acceleration in the laser field, and (iii) recombination with the parent ion and emission of a high energy photon. Therefore, photons could not be generated if ionization could not take place (due to the depletion of the ground state). In other words, if depletion occurs too rapidly, effective interaction could only occur during the very front rising edge of the laser pulse. Therefore, the HHG process would not be effective if the DP intensity is much higher than the ionization saturation intensity.

Figures 2(b)–2(d) show the calculated harmonic spectra in Ag, Ag^+, and Ag^{2+} at different DP intensities using Lewenstein's model. In the calculation, the GSZ potential of different parameters is used to mimic different ions.[31] The laser pulse has a flat-top shape with a two-cycle ramp up. As shown in Fig. 2(b), no visible harmonic peaks are seen from Ag within the energy range of our interest due to the aforementioned problem of ionization depletion. A similar problem existed in the case of Ag^+ when the DP intensity is at 3×10^{14} W/cm^2 or above [shown in Fig. 2(c)]. On the other hand, however, for Ag^{2+}, if the DP intensity is too low, then the ionization probability is also too low to support HHG. But as the intensity is increased to higher than 2×10^{14} W/cm^2, many high order harmonics are generated. From these results, it appears that the contribution of Ag atoms, Ag^+ and Ag^{2+} to the measured harmonics spectra is dependent on the DP intensity. At $I_{fs} = 0.6 \times 10^{14}$ W/cm^2, the harmonics are generated due to the contribution of Ag^+, and the contribution of Ag^+ dominated up to $I_{fs} = 2.4 \times 10^{14}$ W/cm^2. Ag^{2+} contribution initiated at 1.8×10^{14} W/cm^2 having the harmonic spectra 31H to 57H, with further increase in I_{fs} up to 4.8×10^{14} W/cm^2 the harmonics spectra are expanded toward higher cutoff, as marked in Fig. 2(c). The obtained harmonic cutoff for Ag bulk and the theoretical cutoff for Ag atom, Ag^+ and Ag^{2+}, is shown in Fig. 3. It is observed that the experimental cutoff is about half of theoretical cutoff obtained from simulations for Ag^+ and Ag^{2+} ions at various values of I_{fs}. It might be possible that the main influence to the restriction of cut-off energy was instigated by the self-defocusing of DP.[32]

Studying the influence of the DP ellipticity (ε) to the HHG spectrum also reveals the contributions of different ions. The DP ellipticity (ε) is defined as the ratio between the field amplitude of the two orthogonal components of the laser field, that is, $\varepsilon = E_{xo}/E_{yo}$, where $\vec{E}(t) = E_{xo}\cos\omega t\ \hat{x} + E_{yo}\sin\omega t\ \hat{y}$. Figure 4(a) shows the harmonic spectrum as a function of ε (with fixed DP and HP intensities $I_{fs} = 4.5 \times 10^{14}$ W/cm^2; $I_{ps} = 7.5 \times 10^9$ W/cm^2). As expected, it was found that the intensity of all harmonics decreases as the magnitude of ε increases from zero. From Fig. 4(a), we have taken the yield of each harmonic as a function of ε and applied Gaussian fits to the intensity of harmonics-vs-ε data for each harmonic and obtained the half-width-at-half-maximum (HWHM) values of the fitted curves. Here, we refer to the fitted HWHM value as the threshold ellipticity ε_{th}. Physically, threshold ellipticity (ε_{th}) denotes the ellipticity value at which the generated

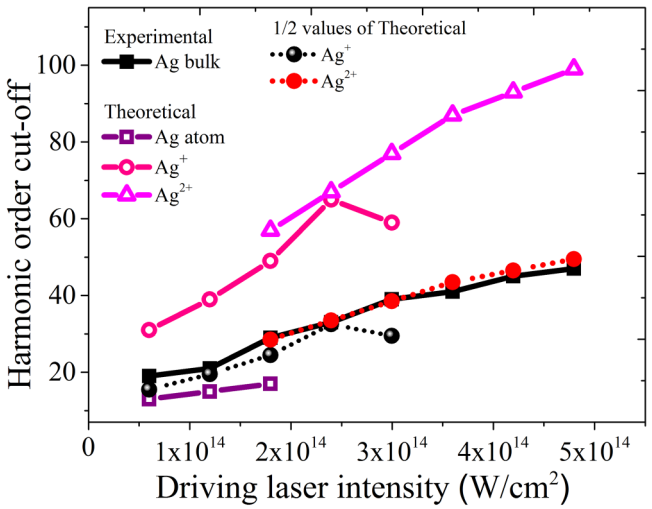

FIG. 3. Experimental and theoretical harmonic cutoffs obtained from Fig. 2.

harmonic yield is half of the yield in the case of a linearly polarized driving field. Figure 4(b) shows the fitted values of ϵ_{th} as a function of harmonic order for Ag bulk (spheres with the solid line). The overall trend of decrease is the indication of the properties of classical dynamics of electron recollision.

The theoretical values of ϵ_{th} with respect to harmonic energy using a semi-classical formulation reported in Ref. 33 by assuming that calculated harmonics are mainly contributed by the short quantum trajectories. In brief, the procedure is to first calculate the excursion times of the electron trajectories for each return energy and then evaluate the corresponding values of ϵ_{th} under the assumption that the distribution of initial transverse momentum of the electron $p_{\perp 0}$ is given by the Perelomov–Popov–Terentev (PPT) theory of strong-field ionization.[28] Three sets of calculated results are presented in Fig. 4(b), one is for harmonics generation from Ag atoms (short dotted line), the second one is singly charged silver ions (solid line), and the other is for doubly ionized silver (dotted-dashed line). Overall agreement between experiment and theory for ions is observed, and the fact that the agreement is better with the calculations for ions supports the assumption that the measured harmonics between 15H-24H and 27H-47H are indeed mainly contributed by Ag^{+} for and Ag^{2+}, respectively. In addition, from

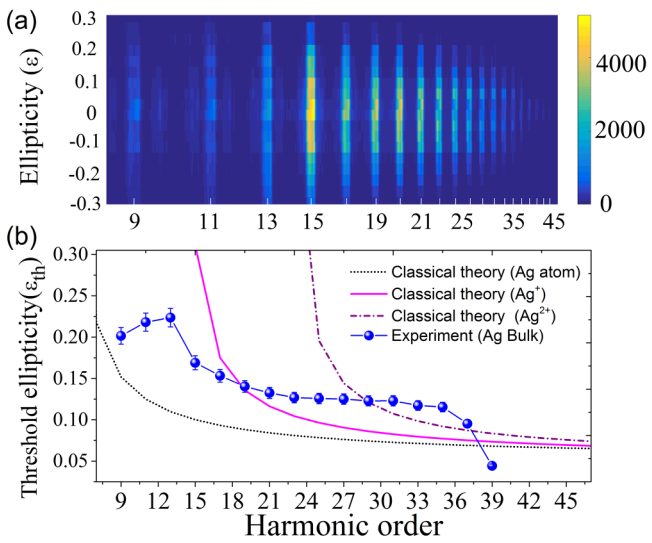

FIG. 4. (a) Harmonic spectrum from Ag plasma as a function of DP ellipticity and (b) threshold ellipticity as a function of harmonic order. Filled sphere: fitted values from experiments. Predictions from the classical calculations for Ag atoms (dotted line), Ag+ ions (solid line), and Ag^{2+} ions (short dashed-dotted line).

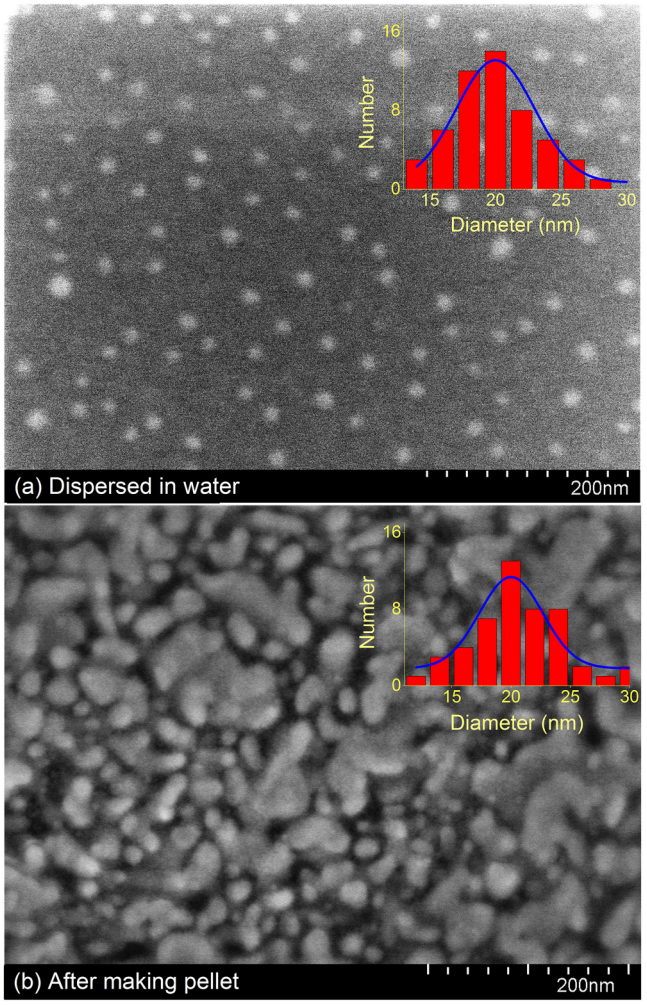

FIG. 5. SEM images of Ag NPs: (a) dispersed on a flat substrate and (b) after being compressed to form a pellet-shaped target. The insets show the size distribution range of nanoparticles.

calculations of strong-field ionization probability, we also expect that Ag atoms would not contribute significantly in the higher-order range (15H-47H) of the measured spectrum.

B. Comparison between the HHG in the LIPs of bulk Ag bulk and Ag NPs

1. Morphology of the NP sample

We used commercially available (purity >99.95%) NP powders of a spherical shape. To inspect the nanoparticles, we used them to prepare a solution and then coated it on a silicon substrate for SEM imaging. Figure 5(a) shows SEM images of the NPs on the silicon substrate. The histogram shows the diameter distribution of the NPs in the image, which is ranged between ~10 and 30 nm with a mean value of 20 nm.

The target samples for the HHG experiments were prepared by using a hydraulic press to compress the NP powders to form a pellet of a diameter of 10 mm and a thickness of 1 mm. Unlike previous studies where the samples were prepared by mixing NPs with polymers (glue), this method ensures that the LIP is free of unwanted substances from the polymers. Figure 5(b) shows an SEM image of the sample surface. It can be seen that some NPs are aggregated due to the external pressure applied. However, majority of NPs well separated and having a mean size of ~20 nm.

2. Harmonics spectra produced from LIP ablated by picoseconds pulses

Figures 6(a)–6(f) show the harmonics spectra comparison between bulk and NPs of silver at three different DP (at fixed $I_{ps} = 7.4 \times 10^9$ W/cm^2) and HP (at fixed $I_{fs} = 4.8 \times 10^{14}$ W/cm^2) intensities, respectively. The higher order harmonics (i.e., >33H) present only when I_{fs} is at least 3.0×10^{14} W/cm^2. The intensities of 9H and 11H for NPs LIPs have almost 3.5 and 1.5 times higher than bulk at $I_{fs} = 0.6 \times 10^{14}$ W/cm^2. The harmonics yields from NPs are considerably higher compared to bulk in most cases, especially for high orders. Figure 7(a) compares the yield of 9H, 15H, and 33H between bulk and NPs with respect to different intensities of DP. It is known that the intensity of the harmonic is proportional to the density of plasma plumes. Therefore, by considering the intensities of harmonics, it is assumed that during the laser ablation NPs forms denser plasma than bulk. Meanwhile, at $I_{fs} = 4.8 \times 10^{14}$ W/cm^2, the harmonics intensities from 9H to 49H are relatively stronger for NPs (cutoff 49H) than Ag bulk (cutoff 47H), and NPs harmonics spectra show a plateau pattern from 9H to 43H. Therefore, at $I_{fs} = 4.8 \times 10^{14}$ W/cm^2, the contribution of HHG mainly from Ag^{2+}, which also supports by theoretical simulation harmonic spectra shown in Fig. 2(d). At a fixed DP intensity ($I_{fs} = 4.8 \times 10^{14}$ W/cm^2), we further study the dependence of harmonic intensities as a function of ps HP intensity between 1.8×10^9 and 1.2×10^{10} W/cm^2. Figures 6(d)–6(f) show the HHG spectra from Ag bulk and NPs at three different HP intensities. It is interesting to note that at a lower intensity of HP, the NP LIP generates stronger harmonics (almost ten times) than bulk. It is likely because the NP ejection and plasma plume density is higher from NP target. Figure 7(b) shows the 15H yield for bulk and NPs, and their intensity ratios (NPs/bulk) as a function of I_{ps}. It clearly indicates that the harmonic yield of NPs is higher than that of bulk. However, the ratio between the harmonics yields gradually decrease (shown in Fig. 7(b), right panel:

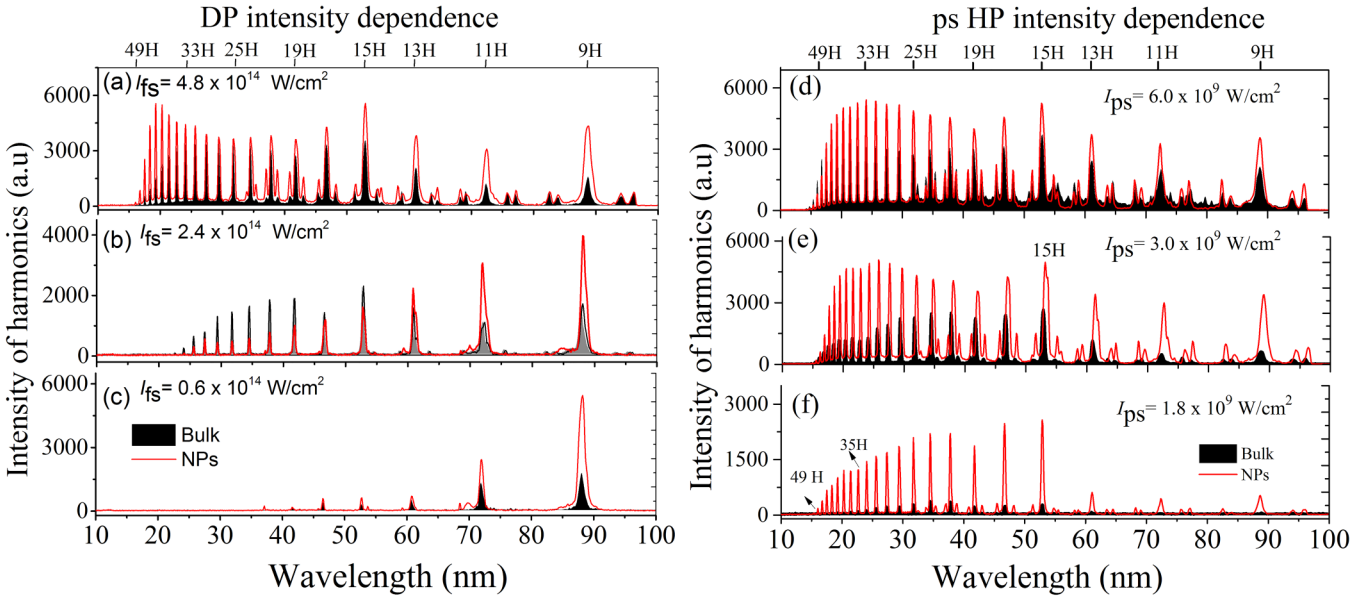

FIG. 6. Harmonics spectra from the plasmas of Ag bulk and 20 nm NPs with DP intensity (I_{fs}) at (a) 4.8×10^{14} W/cm^2, (b) 2.4×10^{14} W/cm^2, and (c) 0.6×10^{14} W/cm^2 at a fixed $I_{ps} = 7.4 \times 10^9$ W/cm^2, for at ps HP intensities (I_{ps}) at (d) 6.0×10^9 W/cm^2, (e) 3.0×10^9 W/cm^2, and (f) 1.8×10^9 W/cm^2, at a fixed $I_{fs} = 4.8 \times 10^{14}$ W/cm^2, respectively.

spheres with solid line) as I_{ps} increases. The harmonics yield saturates after $\sim I_{ps} = 6.0 \times 10^9$ W/cm^2 for both targets. The solid lines represent exponential fits using the equation $y = y_o - A_1 \exp\left(-\frac{x}{t_1}\right)$ of data points for bulk and NPs, respectively. The targets ablating with higher intensities likely lead to more free electrons in the plasma plume, which limited the HHG efficiency. Therefore, the enhancement in the harmonics yield does not further increase. Meanwhile, NPs LIP induces 1.2 and 2.5 times higher intensity at 11.85×10^9 W/cm^2 and 3.0×10^9 W/cm^2, respectively, than the bulk LIP. Figure 7(c) shows the obtained cutoff for NPs compared to bulk (data taken from Fig. 3). The harmonic cutoff is increased with intensity of DP and it is almost the same for both samples (~2 orders high for NPs).

Also, we measure HHG spectrum as a function of driving ellipticity and extract as a function of harmonic order, as shown in Fig. 7(d). The results from the bulk Ag are also plotted together for comparison. The behavior is similar to each other for most of the harmonic orders.

3. Harmonics spectra produced from LIP ablated by nanoseconds pulses

The characteristics and dynamics of LIPs are extremely reliant on laser pulse duration, since it strongly affects the process of energy absorption, heating, and ablation. According to previous studies,[34–36] the spatial–temporal distribution of the plasma plumes

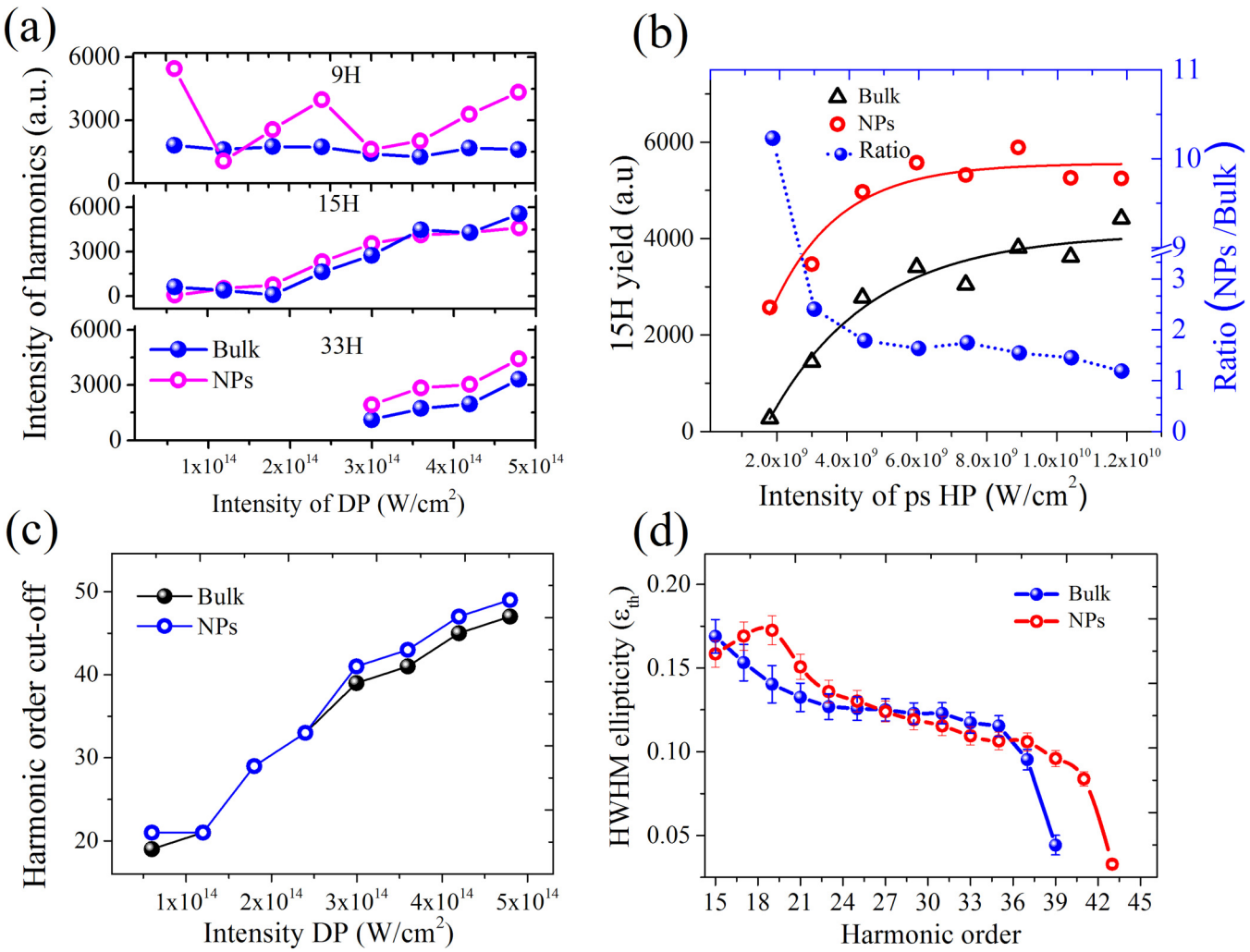

FIG. 7. (a) Yield of 9H, 15H, and 33H for Ag bulk and 20 nm NPs as a function of DP intensity; (b) 15H yield for bulk and NPs, and ratio (NPs/bulk) of 15H as a function of HP intensity, red and black solid lines represent the exponential fits; (c) harmonic cutoff energy as a function of DP intensity for bulk and NP target; and (d) harmonics spectra as a function of threshold ellipticity, spheres, and open circles with solid line represents experimental data for Ag bulk and 20 nm NPs.

produced by long laser pulses are distinctively different from that of the plumes produced by short laser pulses. For instance, Verhoff *et al.*[34] showed that fs LIP exhibited narrower angular distribution of ions and evaporated mass in comparison with ns LIPs. That is, the plasma expansion angle in the case of fs ablation is smaller than plasma produced by ns pulses.

Figure 8 shows the harmonic spectra from LIP of bulk and NPs recorded at intensities of DP, $I_{fs} = 1.8 \times 10^{14}$ W/cm^2 and HP $I_{ns} = 4.2 \times 10^{10}$ W/cm^2 with various delays between the HP and DP. An obvious common feature is that the cutoffs of the harmonic spectra are significantly lower than the case of ps HP presented in Sec. II. It could be treated as an indication that the ion density of LIP produced by long pulses is indeed significantly lower than that by short pulses, as mentioned. Nevertheless, the harmonic yield from Ag NPs is still significantly higher than that from bulk Ag.

The yields of 11H as a function of delay for both targets are shown in Fig. 9. The harmonic yield is peaked at 400 ns delay for both cases. It is noteworthy that not only the yield from the NPs is higher, but also it is extended up to longer delays (up to ~1500 ns) compared to bulk Ag (up to ~800 ns). We believe that the extension of the delay time is an indication of the presence of a significant number of NPs in the plasma plume. Typically, LIPs from solids not only contain isolated atoms and ions (monomers) but also contains some clusters of atoms or NPs. However, compared with monomers, the emission of NPs usually happens later, and their emission velocities are also slower. Therefore, the harmonics-generated at a longer delay time (a few hundred nanoseconds or longer) should be mainly contributed by nanoparticles in the plasma plume. Therefore, the fact that HHG from the LIP of NP sample survive at a longer delay time (and higher yield) compared with bulk sample is evidence which indicates that the number of NPs in the LIP generated from NP sample is significantly greater than that in the LIP from the bulk sample.

In both cases, the maximum harmonic yield is obtained at 400 ns delay, which implies that a large portion of the particles in the plasma plume arrive at the focal point of the DP at that time. The velocity of this group of particles could be estimated simply by dividing the lateral distance between the DP and the sample surface (0.2 μm) by the delay value, which gives 0.5×10^3 m/s. It is close to the value obtained in a previous HHG study.[17] The calculated velocities at different delay times for a fixed distance of 0.2 μm is shown in the inset of Fig. 9.

The harmonic yields are analyzed in the range of 100–1500 ns delays, which were significantly higher within the 200–800 ns range for NPs. In the case of both targets between delay range of 100–800 ns, our observations it indicates that at optimal ablation of atoms and clusters, the laser-induced plasmas produced on the surfaces of different silver contained species spread out from targets with the comparable velocities. Between 900 and 1500 ns delay range, HHG spectra of NPs indicates that, during the laser ablation of NPs comparable high sized clusters of nanoparticles are produced than the bulk ablation and which are responsible for the generation of harmonics.

Figures 10(a) and 10(b) show HHG from plasma plume (at 400 ns delay) of bulk and NPs at $I_{ns} = 4.18 \times 10^{10}$ W/cm^2 with respect to $I_{fs} = 1.8 \times 10^{14}$ W/cm^2 and 4.2×10^{14} W/cm^2. It was observed that at $I_{fs} = 1.8 \times 10^{14}$ W/cm^2 the harmonics is limited to

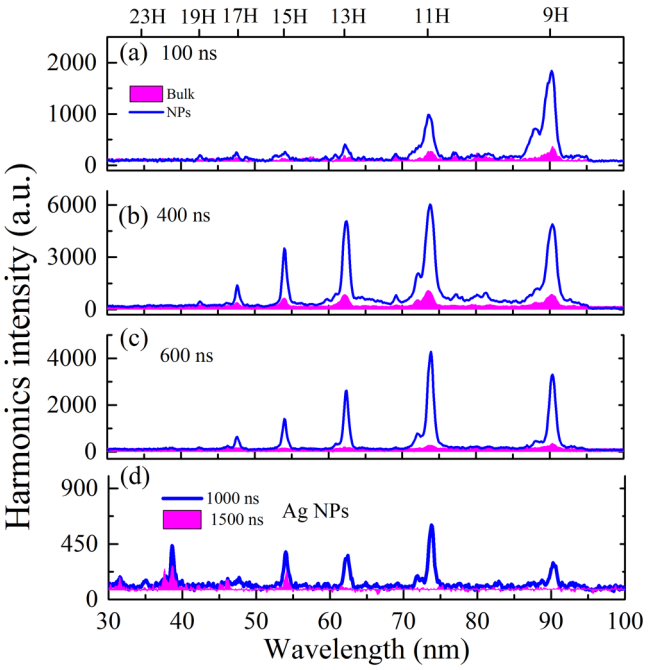

FIG. 8. Harmonic spectra from the plasmas of bulk Ag and Ag 20 NPs for some of the delays between ns HP-fs DP at (a) 100 ns, (b) 400 ns, (c) 600 ns, and only for Ag 20 NPs (d) at 1000 ns and 1500 ns delays, at $I_{fs} = 1.8 \times 10^{14}$ W/cm^2, $I_{ns} = 4.18 \times 10^{10}$ W/cm^2.

19H (42.1 nm) and extended up to 25H (32 nm) for Ag NPs at $I_{fs} = 4.8 \times 10^{14}$ W/cm^2 at similar $I_{ns} = 4.18 \times 10^{10}$ W/cm^2. Figures 10(c) and 10(d) show HHG spectra from plasma plume of bulk and NPs at I_{fs} 4.8×10^{14} W/cm^2 with respect to I_{ns} at 8.3 and

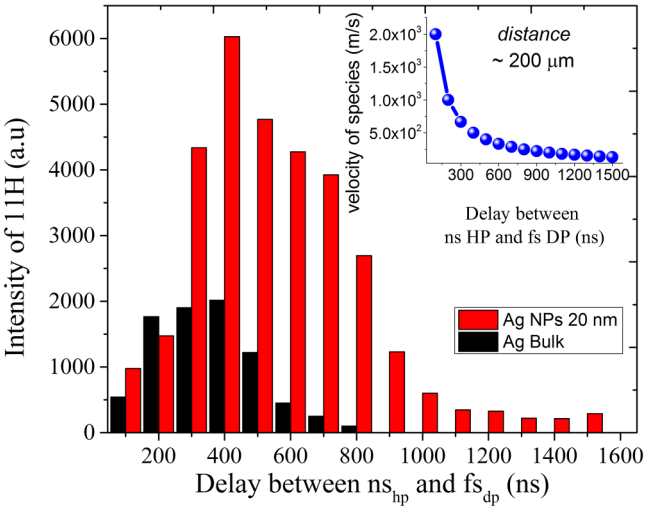

FIG. 9. Dependence of the H11 on the delay between HP and DP.

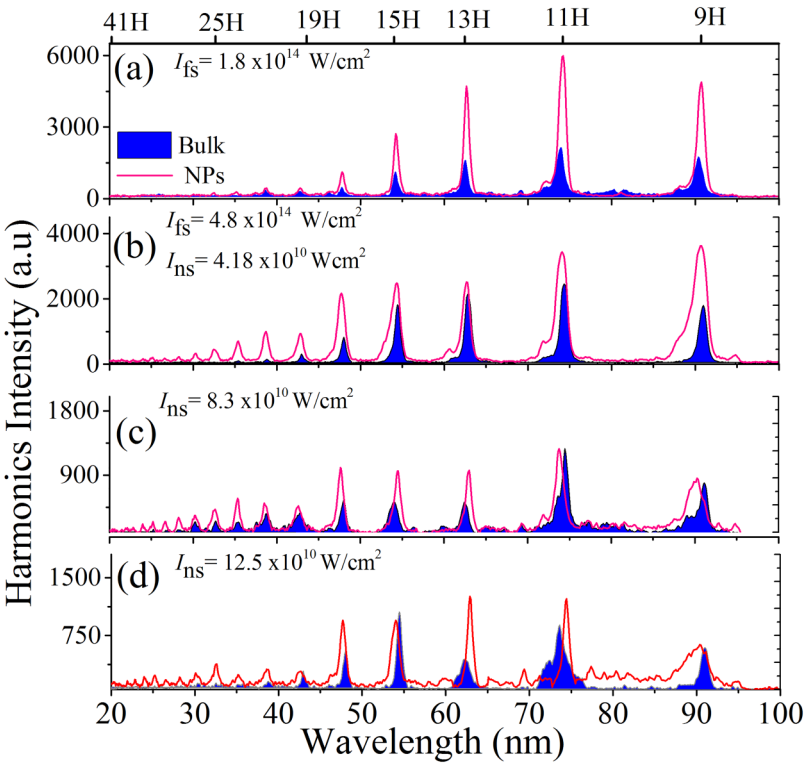

FIG. 10. HHG spectra from LIP (at 400 ns delay) of bulk, 20 nm NPs at $I_{ns} = 4.8 \times 10^{10}$ W/cm^2 for DP intensity at (a) $I_{fs} = 1.8 \times 10^{14}$ W/cm^2, (b) $I_{fs} = 4.8 \times 10^{14}$ W/cm^2, and at $I_{fs} = 4.8 \times 10^{14}$ W/cm^2 for ns HP intensities (c) $I_{ns} = 8.3 \times 10^{10}$ W/cm^2, (d) $I_{ns} = 12.5 \times 10^{10}$ W/cm^2.

12.5×10^{10} W/cm^2. It was observed that the increment in the I_{ns} the harmonic yields shows decrement as compared to $I_{ns} = 4.18 \times 10^{10}$ W/cm^2. It seems that 4.18×10^{10} W/cm^2 is the threshold intensity of nanoseconds pulses to ablate the silver targets.

It is observed that the plasma produced using ps HP leads to a higher harmonic than the ns HP. At $I_{fs} = 1.8 \times 10^{14}$ W/cm^2 in the case of both ps [Fig. 2(a), 1.8 color panel] and ns LIP [Fig. 10(a)] the intensity of harmonics shows a similar pattern, i.e., 9H intensity is high and further order 11H to high harmonics intensity gets lower. As we mentioned above, the ns LIP plumes possess spherical expansion, whereas ps LIP plumes are close to the cylindrical expansion with narrower angular distribution of ions. Moreover, the beam size of the ps_{hp} (71 μm) is higher than ns_{hp} (34.5 μm) and the interaction length between the DP and plasma is longer in the case of ps LIP. Therefore, in the case of ps LIP, there is a high probability of excitation of a higher density of ions. ns LIP contains more number of Ag atoms than ions. Therefore, a higher cutoff and maximum yield is obtained for ps LIPs. Based on quantum mechanical simulations, it is obtained that the Ag atom produces lower-order harmonics, and Ag+ and Ag^{2+} ions lead to extension of the higher orders. Also, it is important to notice that the intensity of harmonics for silver NPs is considerable higher than bulk Ag and this is consistent with the results in Ref. 37.

IV. CONCLUSION

We have demonstrated the experimental and theoretical approach for responsible plasma components for the generation of higher-order harmonics using 800 nm, 35 fs driving laser pulses. The study consists of optimal driving pulse intensity and ellipticity of driving pulse describes the contribution of Ag atoms, Ag^+ and Ag^{2+} ions, toward the generation of HHG spectra from silver plasma. Furthermore, we have made a systematic comparison between HHG produced from plasma plumes of Ag bulk and 20 nm NPs. This indicates that the tunability of harmonics can be achieved between 9H-19H, middle (15H-35H), and total harmonics (9H-49H) of HHG spectra from LIP of bulk and NPs, by varying the driving and heating pulse intensities. In the case of ps LIP, the order of the harmonics extended up to the 49H (16.32 nm) of DP. In both cases of LIP by ps and ns, it is found that the harmonic yield and cutoff of harmonics are suggestively improved for NPs as compared to the bulk material. In the case of ns LIP, the harmonic cutoff is extended to 41H, however, the harmonics yield is higher for the lower-order region (9H-17H) than the 19H-41H. The Ag bulk produced the harmonics spectra up to 800 ns, whereas the NPs extended delays until 1.5 μs, and both samples have maximum intensity at 400 ns delay, which is an indication that the LIP generated from the NP samples contains significantly more NPs compared with the LIP from the bulk sample.

ACKNOWLEDGMENTS

K. S. Rao acknowledges support by the Chinese Academy of Sciences President's International Fellowship Initiative (Grant No. 2021PM0036). This work is supported by the National Natural Science Foundation of China (Grant No. 12004380), Jilin

Provincial Science & Technology Development Project (Grant No. YDZJ202102CXJD002), and the K. C. Wong Education Foundation (Grant No. GJTD-2018-08). Also, K. S. Rao would like to thank Professor Rashid A. Ganeev for initial discussions on HHG studies. Y. H. Lai would like to thank Professor Xu Wang for sharing the code for HHG Lewenstein model simulations.

DATA AVAILABILITY

The data that support the findings of this study are available from the corresponding author upon reasonable request.

REFERENCES

[1]Z. Chang and P. Corkum, J. Opt. Soc. Am. B **27**, B9 (2010).
[2]T. Popmintchev, M.-C. Chen, P. Arpin, M. M. Murnane, and H. C. Kapteyn, Nat. Photonics **4**, 822 (2010).
[3]F. Krausz and M. Ivanov, Rev. Mod. Phys. **81**, 163 (2009).
[4]F. Corkum and P. B. Krausz, Nat. Phys. **3**, 381 (2007).
[5]J. Li, J. Lu, A. Chew, S. Han, J. Li, Y. Wu, H. Wang, S. Ghimire, and Z. Chang, Nat. Commun. **11**, 2748 (2020).
[6]R. A. Ganeev, M. Suzuki, M. Baba, M. Ichihara, and H. Kuroda, J. Appl. Phys. **103**, 063102 (2008).
[7]R. A. Ganeev, J. Opt. Soc. Am. B **31**, 2221 (2014).
[8]H. Singhal, P. A. Naik, M. Kumar, J. A. Chakera, and P. D. Gupta, J. Appl. Phys. **115**, 033104 (2014).
[9]M. A. Fareed, V. V. Strelkov, N. Thiré, S. Mondal, B. E. Schmidt, F. Légaré, and T. Ozaki, Nat. Commun. **8**, 16061 (2017).
[10]L. B. Elouga Bom, S. Haessler, O. Gobert, M. Perdrix, F. Lepetit, J.-F. Hergott, B. Carré, T. Ozaki, and P. Salières, Opt. Express **19**, 3677 (2011).
[11]Y. Pertot, S. Chen, S. D. Khan, L. B. E. Bom, T. Ozaki, and Z. Chang, J. Phys. B: At. Mol. Opt. Phys. **45**, 074017 (2012).
[12]N. Rosenthal and G. Marcus, Phys. Rev. Lett. **115**, 133901 (2015).
[13]R. A. Ganeev, G. S. Boltaev, V. V. Kim, M. Iqbal, H. Kuroda, and A. S. Alnaser, J. Appl. Phys. **129**, 043103 (2021).
[14]R. A. Ganeev, S. Odžak, D. B. Milošević, M. Suzuki, and H. Kuroda, Laser Phys. **26**, 075401 (2016).
[15]R. A. Ganeev, T. Witting, C. Hutchison, V. V. Strelkov, F. Frank, M. Castillejo, I. Lopez-Quintas, Z. Abdelrahman, J. W. G. Tisch, and J. P. Marangos, Phys. Rev. A **88**, 033838 (2013).
[16]V. Strelkov, Phys. Rev. Lett. **104**, 123901 (2010).
[17]R. A. Ganeev, V. V. Kim, K. S. Rao, and C. Guo, Appl. Sci. **11**, 2143 (2021).
[18]R. A. Ganeev, M. Suzuki, S. Yoneya, and H. Kuroda, J. Appl. Phys. **117**(2), 023114 (2015).
[19]J. A. Chakera, H. Singhal, R. A. Ganeev, P. A. Naik, A. K. Srivastav, A. Singh, R. Chari, A. Khan, and P. D. Gupta, AIP Conf. Proc. **1228**, 413 (2010).
[20]M. Masnavi, M. Nakajima, K. Horioka, H. P. Araghy, and A. Endo, J. Appl. Phys. **109**, 123306 (2011).
[21]R. A. Ganeev, G. S. Boltaev, V. V. Kim, M. Venkatesh, A. I. Zvyagin, M. S. Smirnov, O. V. Ovchinnikov, M. Wöstmann, H. Zacharias, and C. Guo, J. Appl. Phys. **126**, 193103 (2019).
[22]R. A. Ganeev, H. Singhal, P. A. Naik, U. Chakravarty, V. Arora, J. A. Chakera, R. A. Khan, M. Raghuramaiah, S. R. Kumbhare, R. P. Kushwaha, and P. D. Gupta, Appl. Phys. B **87**, 243 (2007).
[23]R. A. Ganeev, M. Suzuki, M. Baba, and H. Kuroda, Phys. Rev. **76**, 023805 (2007).
[24]R. A. Ganeev, M. Baba, M. Suzuki, and H. Kuroda, Phys. Lett. A **339**, 103 (2005).
[25]R. A. Ganeev, L. B. Elouga Bom, and T. Ozaki, J. Phys. B: At. Mol. Opt. Phys. **42**, 055402 (2009).
[26]R. A. Ganeev, M. Suzuki, M. Baba, M. Ichihara, and H. Kuroda, J. Phys. B: At. Mol. Opt. Phys. **41**, 045603 (2008).
[27]H. Singhal, R. A. Ganeev, P. A. Naik, A. K. Srivastava, A. Singh, R. Chari, R. A. Khan, J. A. Chakera, and P. D. Gupta, J. Phys. B: At. Mol. Opt. Phys. **43**, 025603 (2010).
[28]A. M. Perelomov, V. S. Popov, and M. V. Terent'ev, Sov. Phys. JETP **23**, 924 (1966).
[29]Y. H. Lai, J. Xu, U. B. Szafruga, B. K. Talbert, X. Gong, K. Zhang, H. Fuest, M. F. Kling, C. I. Blaga, P. Agostini, and L. F. Dimauro, Phys. Rev. A **96**, 063417 (2017).
[30]P. Balcou, M. Y. Ivanov, A. L. Huillier, and P. B. Corkum, Phys. Rev. A **49**, 2117 (1994).
[31]R. H. Garvey, C. H. Jackman, and A. E. S. Green, Phys. Rev. A **12**, 1144 (1975).
[32]R. A. Ganeev, M. Baba, M. Suzuki, and H. Kuroda, Phys. Lett. A **339**, 103 (2005).
[33]V. V. Strelkov, M. A. Khokhlova, A. A. Gonoskov, I. A. Gonoskov, and M. Y. Ryabikin, Phys. Rev. A **86**(1), 013404 (2012).
[34]B. Verhoff, S. S. Harilal, J. R. Freeman, P. K. Diwakar, and A. Hassanein, J. Appl. Phys. **112**, 093303 (2012).
[35]S. S. Mao, X. Mao, R. Greif, and R. E. Russo, Appl. Phys. Lett. **77**, 2464 (2000).
[36]S. Gurlui, M. Agop, P. Nica, M. Ziskind, and C. Focsa, Phys. Rev. E **78**, 026405 (2008).
[37]R. A. Ganeev, C. Hutchison, F. Mcgrath, D. Y. Lei, M. Castillejo, and J. P. Marangos, Phys. Rev. A **88**, 033803 (2013).